AMERICAN SOCIETY FOR MICROBIOLOGY | Journal of Bacteriology®

RESEARCH ARTICLE

Optogenetic Manipulation of Cyclic Di-GMP (c-di-GMP) Levels Reveals the Role of c-di-GMP in Regulating Aerotaxis Receptor Activity in *Azospirillum brasilense*

Lindsey O'Neal,[a] Min-Hyung Ryu,[b]* Mark Gomelsky,[b] Gladys Alexandre[a]

Department of Biochemistry, Cellular and Molecular Biology, University of Tennessee, Knoxville, Tennessee, USA[a]; Department of Molecular Biology, University of Wyoming, Laramie, Wyoming, USA[b]

ABSTRACT Bacterial chemotaxis receptors provide the sensory inputs that inform the direction of navigation in changing environments. Recently, we described the bacterial second messenger cyclic di-GMP (c-di-GMP) as a novel regulator of a subclass of chemotaxis receptors. In *Azospirillum brasilense*, c-di-GMP binds to a chemotaxis receptor, Tlp1, and modulates its signaling function during aerotaxis. Here, we further characterize the role of c-di-GMP in aerotaxis using a novel dichromatic optogenetic system engineered for manipulating intracellular c-di-GMP levels in real time. This system comprises a red/near-infrared-light-regulated diguanylate cyclase and a blue-light-regulated c-di-GMP phosphodiesterase. It allows the generation of transient changes in intracellular c-di-GMP concentrations within seconds of irradiation with appropriate light, which is compatible with the time scale of chemotaxis signaling. We provide experimental evidence that binding of c-di-GMP to the Tlp1 receptor activates its signaling function during aerotaxis, which supports the role of transient changes in c-di-GMP levels as a means of adjusting the response of *A. brasilense* to oxygen gradients. We also show that intracellular c-di-GMP levels in *A. brasilense* change with carbon metabolism. Our data support a model whereby c-di-GMP functions to imprint chemotaxis receptors with a record of recent metabolic experience, to adjust their contribution to the signaling output, thus allowing the cells to continually fine-tune chemotaxis sensory perception to their metabolic state.

IMPORTANCE Motile bacteria use chemotaxis to change swimming direction in response to changes in environmental conditions. Chemotaxis receptors sense environmental signals and relay sensory information to the chemotaxis machinery, which ultimately controls the swimming pattern of cells. In bacteria studied to date, differential methylation has been known as a mechanism to control the activity of chemotaxis receptors and modulates their contribution to the overall chemotaxis response. Here, we used an optogenetic system to perturb intracellular concentrations of the bacterial second messenger c-di-GMP to show that in some chemotaxis receptors, c-di-GMP functions in a similar feedback loop to connect the metabolic status of the cells to the sensory activity of chemotaxis receptors.

KEYWORDS *Azospirillum*, c-di-GMP, chemotaxis, aerotaxis

Received 12 January 2017 **Accepted** 28 February 2017

Accepted manuscript posted online 6 March 2017

Citation O'Neal L, Ryu M-H, Gomelsky M, Alexandre G. 2017. Optogenetic manipulation of cyclic di-GMP (c-di-GMP) levels reveals the role of c-di-GMP in regulating aerotaxis receptor activity in *Azospirillum brasilense*. J Bacteriol 199:e00020-17. https://doi.org/10.1128/JB.00020-17.

Editor Ann M. Stock, Rutgers University-Robert Wood Johnson Medical School

Address correspondence to Gladys Alexandre, galexan2@utk.edu.

* Present address: Min-Hyung Ryu, Department of Biological Engineering, Massachusetts Institute of Technology, Cambridge, Massachusetts, USA.

For a companion article on this topic, see https://doi.org/10.1128/JB.00014-17.

The bacterial second messenger cyclic di-GMP (c-di-GMP) has emerged as a key signaling molecule regulating the transition of bacteria from planktonic to sessile lifestyles. In addition to regulating this transition, c-di-GMP signaling pathways control biofilm formation, adhesion to surfaces, virulence, the cell cycle, and other processes (1). Intracellular c-di-GMP levels are set by diguanylate cyclases, which synthesize

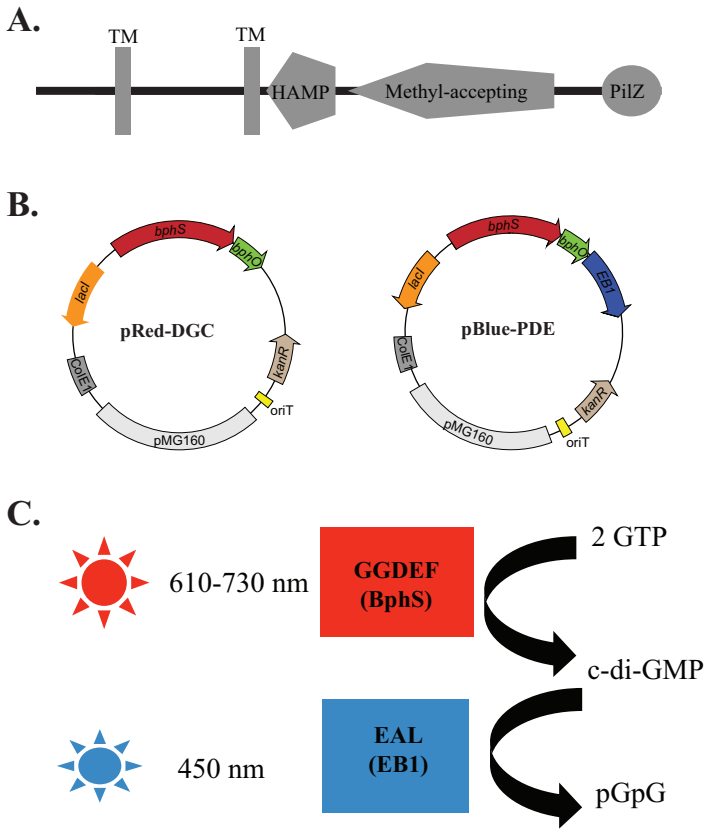

FIG 1 Domain architecture of Tlp1 and dichromatic optogenetic system for manipulating c-di-GMP levels in proteobacteria. (A) Tlp1 is a prototypical chemotaxis receptor comprising an N-terminal sensing domain between two transmembrane (TM) regions exposed to the periplasm followed by a HAMP (histidine kinase, adenyl cyclase, methyl-accepting protein, and phosphatase) domain and a C-terminal signaling methyl-accepting (MA) domain. A PilZ domain is also present at the extreme C terminus of Tlp1. (B) Maps of plasmids pRed-DGC and pBlue-PDE, with pRed-DGC expressing the red-light-activated diguanylate cyclase BphS and pBlue-PDE expressing the blue-light-activated phosphodiesterase EB1. (C) Wavelengths of light used to activate BphS and EB1 activities in order to induce c-di-GMP synthesis and degradation, respectively.

c-di-GMP, and c-di-GMP-dependent phosphodiesterases (PDEs), which degrade c-di-GMP. The diguanylate cyclase activity is encoded by a highly conserved GGDEF domain, while phosphodiesterase activity resides within conserved EAL or HD-GYP domains (1). c-di-GMP effectors that mediate changes in c-di-GMP concentrations come in many forms: transcriptional regulators, riboswitches, metabolic enzymes, and signal transduction proteins (1). The diversity of signal inputs and outputs associated with c-di-GMP signaling and effector proteins reflects the widespread role of this molecule in regulating bacterial metabolism and cellular behaviors.

The PilZ domain represents one of the best-characterized classes of c-di-GMP effectors (1). Binding of c-di-GMP to a PilZ domain changes its conformation and allosterically regulates activities of the output domains linked to it (2–4). A PilZ domain is present at the C terminus of a chemotaxis receptor, Tlp1, from the alphaproteobacterium *Azospirillum brasilense* (2, 5). Except for the presence of PilZ, Tlp1 possesses a prototypical structure of a chemotaxis receptor: an N-terminal membrane-anchored periplasmic domain that encodes the putative sensor region and a highly conserved C-terminal cytoplasmic kinase control module that interacts with the downstream chemotaxis proteins to permit signal transduction (Fig. 1A) (6). Tlp1 functions as an energy sensor. It mediates the ability of *A. brasilense* to navigate in gradients of compounds that affect intracellular energy levels, including oxygen and organic acids (7, 8). Recently, we showed that the PilZ domain of Tlp1 binds c-di-GMP with high affinity, which affects the ability of cells to navigate in oxygen gradients (5).

A. brasilense grows best under microaerophilic conditions. Elevated oxygen concentrations cause stress to which motile cells transiently adapt by clumping, which is presumed to reduce their surface area and limit oxygen diffusion (9). Furthermore, the addition or removal of air in free-swimming cells triggers rapid (on the order of a few seconds) and transient changes in intracellular levels of c-di-GMP (5), indicating that oxygen is a major factor regulating c-di-GMP concentrations. Consistent with these observations, the binding of c-di-GMP to the PilZ domain of the Tlp1 chemoreceptor alters the aerotaxis (chemotaxis in gradients of oxygen) response (5). Aerotaxis is the strongest behavioral response in *A. brasilense*. Of 33 putative diguanylate cyclases and 25 phosphodiesterases encoded by the *A. brasilense* genome (10, 11), only 2, ChsA and CdgA, have thus far been functionally characterized (11, 12), and ChsA has been shown to contribute to oxygen-induced changes in intracellular c-di-GMP levels (5).

To date, most strategies for characterizing the role of c-di-GMP in cell physiology have relied on modulating the intracellular c-di-GMP concentrations via single and combinatorial mutations of diguanylate cyclases or phosphodiesterases (e.g., see references 13 and 14). Mutants lacking all enzymes involved in c-di-GMP metabolism have been described (e.g., see references 15–17). A complementary approach involving the use of the constitutive or inducible overexpression of diguanylate cyclases or phosphodiesterase has also been used (e.g., see reference 2). While these experimental approaches allow researchers to observe long-term consequences of increased or decreased c-di-GMP levels, they preclude observations of short-term changes in c-di-GMP levels. However, transient changes in c-di-GMP concentrations, i.e., those occurring on a scale of seconds to minutes, can be profound in magnitude and significant (5, 18, 19).

Here, we use an optogenetic (synthetic photobiology) toolset for manipulating intracellular c-di-GMP levels within a seconds-to-minutes temporal resolution (20, 21), which is compatible with the time scale of chemotaxis signaling. This toolset comprises plasmids expressing a red/near-infrared-light-regulated diguanylate cyclase, BphS (21), and a blue-light-regulated c-di-GMP phosphodiesterase, EB1 (20) (Fig. 1B and C). Using this toolset, we show that transient changes in c-di-GMP levels regulate the sensitivity of cells to oxygen gradients generated by the addition or removal of air. We also show that c-di-GMP binding functions as an activation mechanism for the Tlp1 receptor. Finally, we show that carbon metabolism modulates c-di-GMP levels and imprints chemotaxis receptors with a record of recent metabolic experience that allows them to ultimately adjust their preferred position for aerotactic band formation in oxygen gradients. Our data suggest that binding of c-di-GMP to a subset of chemotaxis receptors adjusts their signaling contribution, permitting cells to continually fine-tune chemotactic responses to their metabolic state.

RESULTS

The optogenetic system permits light-dependent regulation of intracellular c-di-GMP levels. To manipulate c-di-GMP levels in *A. brasilense* with the temporal resolution of seconds to minutes, we adapted the dichromatic optogenetic module for c-di-GMP control recently engineered for *Escherichia coli* (20). This system consists of a chimeric red/near-infrared-light-regulated diguanylate cyclase, BphS (21), and a blue-light-activated c-di-GMP phosphodiesterase, EB1 (20) (Fig. 1B). BphS senses light via the biliverdin IXα chromophore that is produced from heme by the heme oxygenase BphO. BphS is activated by red/far-red light (630 to 710 nm) and inactivated by near-infrared light (750 to 780 nm). It can also be activated by violet light of 400 to 420 nm (21). EB1 senses light via the flavin chromophore and is activated by violet-to-blue light (360 to 450 nm) (20). The engineered *bphS-bphO* operon expressing the diguanylate cyclase (plasmid pRed-DGC) or the *bphS-bphO-eb1* operon expressing both the cyclase and phosphodiesterase (plasmid pBlue-PDE) was cloned downstream of the isopropyl-β-D-thiogalactopyranoside (IPTG)-inducible P_{lac} promoter into a broad-host-range vector, pIND4 (22). The plasmid containing the *bphS-bphO-eb1* operon was initially designed to

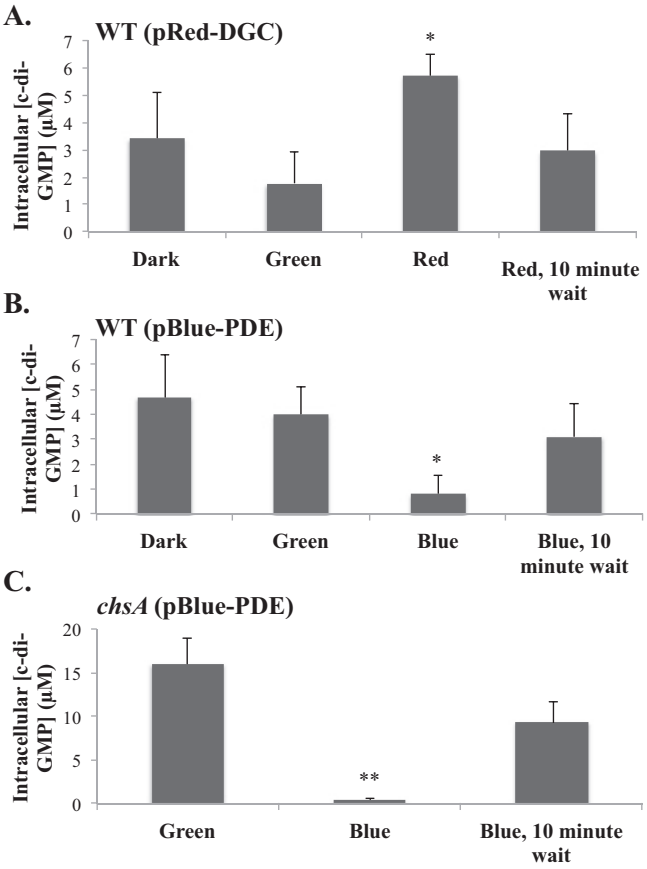

FIG 2 Light-mediated changes in intracellular c-di-GMP concentrations in cells carrying pRed-DGC or pBlue-PDE. (A and B) Changes in intracellular c-di-GMP concentrations in wild-type (WT) cells expressing a red-light-activated diguanylate cyclase [WT(pRed-DGC)] (A) or in wild-type cells containing a plasmid with both a red-light-activated diguanylate cyclase and a blue-light-activated phosphodiesterase [WT(pBlue-PDE)] (B). (C) Changes in intracellular c-di-GMP concentrations in a *chsA* mutant strain carrying the dually red-light-activated diguanylate cyclase and blue-light-activated phosphodiesterase [*chsA*(pBlue-PDE)]. Exposure to the light color indicated on the *x* axis was done for 10 s except for the controls, dark and green light, which correspond to conditions under which the samples were maintained. Quantifications are the averages of data from three biological replicates with standard errors of the means. *, *P* value of <0.05; **, *P* value of <0.01 (between treatment and the control [green light]).

provide the ability to control both c-di-GMP synthesis and degradation, with light, from a single plasmid (Fig. 1B).

We transferred the corresponding plasmids into the *A. brasilense* wild-type (WT) strain and measured changes in intracellular c-di-GMP concentrations in cells exposed to green (505 to 575 nm), red (610 to 730 nm) or blue (450 nm) light (Fig. 1C). Green light does not activate the diguanylate cyclase or the phosphodiesterase, based on the absorption spectra for these enzymes (20). As expected, we found that the intracellular c-di-GMP concentration of cells maintained in the dark did not significantly change when they were exposed to green light (Fig. 2). Given that our experimental approach relies on the real-time observation of free-swimming cells and on the analysis of changes in motility patterns that occur within seconds, we initially tested the effect of pulses of red or blue light exposure ranging from 10 s to 1 min on c-di-GMP concentrations. This initial screening of optimum conditions showed that a 10-s exposure to red or blue light was sufficient to induce statistically significant changes in intracellular c-di-GMP concentrations. Wild-type cells carrying pRed-DGC and maintained under green light had basal levels of c-di-GMP that were immediately increased almost 3-fold upon exposure to red light (Fig. 2A). Under green light conditions, cells carrying the vector expressing both the red-light-activated diguanylate cyclase and the blue-light-

activated phosphodiesterase (pBlue-PDE) had basal levels of c-di-GMP that were significantly decreased upon exposure to blue light (Fig. 2B). No further increase of intracellular c-di-GMP concentrations beyond basal levels could be observed when these cells were exposed to red light (data not shown), possibly because of high *eb1* expression levels resulting in background phosphodiesterase activity and/or red light extending to near infrared (750 nm) that inactivates the diguanylate activity of BphS. We further confirmed the effect of blue light on intracellular c-di-GMP levels by using a *chsA* mutant derivative of *A. brasilense*. The *chsA* mutant possesses constitutively elevated c-di-GMP levels due to the absence of the ChsA phosphodiesterase (5, 11). The expression of the pBlue-PDE vector in this strain background also caused a significant decrease in the intracellular c-di-GMP levels (Fig. 2C). In subsequent experiments, we used pRed-DGC and pBlue-PDE for elevating and lowering intracellular c-di-GMP levels, respectively. The changes in c-di-GMP concentrations induced by light were transient: 10 min after exposure to the inducing light, the intracellular c-di-GMP levels returned to prestimulus levels (Fig. 2). Therefore, we established that the optogenetic system tested here allows the transient manipulation of intracellular c-di-GMP levels in *A. brasilense*.

Optogenetic manipulation of c-di-GMP levels affects aerotaxis. In oxygen gradients generated from the diffusion of air into a cell suspension of free-swimming cells, *A. brasilense* cells are attracted to specific low oxygen concentrations that support their microaerobic metabolism, and they form tight aerotactic bands at these locations (23). The spatial gradient assay for aerotaxis permits the real-time observation of the aerotactic response of motile cells to the gradient. The band pattern (position relative to the air-liquid meniscus and time to formation) is robust and highly reproducible for cells grown under the given conditions (7, 23, 24). An *A. brasilense tlp1* mutant expressing an empty control vector or a Tlp1 variant unable to bind c-di-GMP ($Tlp1^{R562A\ R563A}$) is also affected in its ability to locate the optimum position for metabolism in oxygen gradients (5), suggesting that c-di-GMP metabolism affects aerotaxis. To further test this hypothesis, we used the optogenetic system to modulate intracellular c-di-GMP levels in free-swimming cells exposed to a spatial gradient of air in the capillary assay for aerotaxis (see Fig. S1 in the supplemental material). Under these conditions, cells placed into the capillary tube formed a stable aerotactic band away from the air-liquid interface. Wild-type cells containing pRed-DGC formed a somewhat thicker aerotactic band than that formed by cells carrying pIND4, as a control. Under these conditions, exposure of cells to 10 s of red light did not visibly affect the position or shape of the aerotactic band (Fig. S1A). To test the possible effect of elevated c-di-GMP concentrations on the thickness of the aerotactic band, we exposed these cells to red light repeatedly using two subsequent short pulses of red light to sustain an increase in c-di-GMP levels. In this case, the aerotactic band thickened, and an increase in the density of cell-cell clumps was also observed on the side of the aerotactic band closer to the air-liquid meniscus (Fig. S1B). These observations suggest that as c-di-GMP levels increased, more cells navigated to the aerotactic band, also suggesting that more cells responded to the gradient. The increase in clumping on the side of the band exposed to elevated oxygen concentrations also suggested that the cells experienced an increased sensitivity to oxygen, since the clumping phenotype indicated that these cells were more susceptible to oxygen-induced stress under these conditions. Wild-type cells containing pBlue-PDE also formed an aerotactic band, but it was significantly thinner than that formed by cells carrying pIND4 (Fig. S1C), suggesting that despite being motile, fewer cells responded to the gradient and joined the aerotactic band under these conditions. Decreasing the intracellular c-di-GMP concentration with blue light in cells containing pBlue-PDE did not cause any visible change in the position or shape of the aerotactic band, and no clumping was observed (Fig. S1C). Decreasing the c-di-GMP concentration with blue light in a phosphodiesterase *chsA* mutant, which has constitutively high intracellular c-di-GMP levels (Fig. 2C), completely dissipated the aerotactic band. Returning these cells to green light failed to restore the aerotactic

TABLE 1 Effects of temporal increases in c-di-GMP concentrations on swimming behavior

Light	WT carrying an empty vector		WT(pRed-DGC)	
	Avg swimming speed (μm/s) ± SEM	Avg reversal frequency (s^{-1}) ± SEM	Avg swimming speed (μm/s) ± SEM	Avg reversal frequency (s^{-1}) ± SEM
Green[a]	27 ± 1.5	0.8 ± 0.1	22 ± 1.1	0.9 ± 0.1
Red	24 ± 1.2	0.9 ± 0.1	21 ± 1.2	0.8 ± 0.1
Green[b]	26 ± 1.4	1 ± 0.1	24 ± 1.3	0.8 ± 0.1

[a]Before stimulus with red light.
[b]After stimulus with red light.

band, although some accumulation of cells at the former position of the band could be seen (Fig. S1D). Together, these data suggested that modulating intracellular c-di-GMP levels could alter transient responses in an oxygen gradient.

Next, we wanted to test if changes in c-di-GMP levels using the optogenetic system could modify stable adaptive responses. For this purpose, we used the *chsA* mutant. As we previously reported, free-swimming *chsA* cells swim more slowly than wild-type cells and form many stable aggregates (comprised mostly of nonmotile cells) in cultures (5) (Fig. S2A). The *chsA* mutant carrying the pIND4 or pBlue-PDE vector exposed to noninducing green light formed aggregates in culture (Fig. S2). When exposed to blue light, the density of aggregates within the suspension of *chsA*(pBlue-PDE) cells did not change. Repeated short pulses (10 s each) of blue light did not change this outcome (data not shown). The presence of pBlue-PDE did not significantly decrease the amount of clumps formed in culture (*P* value of 0.1). These data indicate that the transient changes in c-di-GMP levels induced via the optogenetic system were insufficient to alter a more stable adaptive response such as the formation of aggregates.

c-di-GMP levels do not serve as an intracellular attractant or repellent. *A. brasilense* cells respond tactically to oxygen gradients via signaling by two Che systems that coordinately control transient changes in the swimming speed and in the probability of swimming reversals (25, 26). Therefore, we next examined the effect of transient changes in intracellular c-di-GMP levels on these motility parameters under steady-state conditions. We found that a temporal increase in intracellular c-di-GMP concentrations by a short 10-s pulse of red light did not change the swimming speed or the probability of reversals of wild-type cells carrying pRed-DGC, compared to the strain carrying an empty vector, pIND4 (Table 1). Therefore, triggering a temporal increase in c-di-GMP levels in cells carrying pRed-DGC with red light did not cause any change in the motility pattern; i.e., no chemotaxis signaling was induced. Similarly, decreasing the c-di-GMP level using blue light in cells carrying pBlue-PDE did not change these motility parameters. We observed that wild-type cells carrying pBlue-PDE exhibited a significantly lower swimming speed (*P* value of 0.004), regardless of light exposure (Table 2). The reduced swimming speed is not due to a reduced growth rate since the wild-type strain carrying pBlue-PDE has a growth rate of 5.3 ± 1.3 h, which is not statistically different from the growth rate of the wild-type strain carrying pIND4 (4.5 ± 1.0 h). Together, these results demonstrate that c-di-GMP does not directly activate or inhibit chemotaxis signaling; i.e., c-di-GMP does not serve as an intracellular attractant or repellent signal.

TABLE 2 Effects of temporal decreases in c-di-GMP concentrations on swimming behavior

Light	WT carrying an empty vector		WT(pBlue-PDE)[a]	
	Avg swimming speed (μm/s) ± SEM	Avg reversal frequency (s^{-1}) ± SEM	Avg swimming speed (μm/s) ± SEM	Avg reversal frequency (s^{-1}) ± SEM
Green[b]	27 ± 1.8	0.8 ± 0.1	16 ± 1.5*	0.6 ± 0.1
Blue	31 ± 4.4	0.6 ± 0.1	16 ± 0.8*	0.5 ± 0.1
Green[c]	25 ± 1.9	0.8 ± 0.1	16 ± 1.2*	0.4 ± 0.03

[a]* indicates a significant difference compared to uninduced cells under green light conditions ($P < 0.05$ by a *t* test).
[b]Before stimulus with blue light.
[c]After stimulus with blue light.

c-di-GMP levels modulate the ability of cells to detect the preferred oxygen concentration in a spatial gradient of air. Although c-di-GMP does not directly activate changes in swimming motility patterns that would result from chemotaxis signaling, the data described above as well as from our previous work (5) suggest that changes in c-di-GMP levels modulated the ability of cells to sense and/or respond to oxygen gradients. To test this hypothesis further, we exposed cells containing pRed-DGC or pBlue-PDE to inducing light prior to exposing them to the oxygen gradient (see Materials and Methods). As a control, cells were stimulated with noninducible green light. When wild-type cells carrying pRed-DGC were maintained under green light, they started forming an aerotactic band at some distance from the meniscus within 30 s of exposure to the gradient, with a stable aerotactic band being established 40 s after exposure to the gradient. The formation of the band at this position and within this time frame is highly reproducible in cultures grown under similar conditions. Increasing c-di-GMP levels in these cells prior to exposing them to the oxygen gradient caused a reproducible and consistent lag of about 10 s, with a stable aerotactic band being formed by 60 s after exposure to the gradient (Fig. 3A).

Wild-type cells carrying pBlue-PDE and exposed to noninducing green light prior to being exposed to the oxygen gradient formed a very faint and narrow aerotactic band 140 s after the introduction of the gradient, despite the cells being motile (Fig. 3B). Incubation of these cells for longer times did not cause band widening (data not shown). Decreasing the c-di-GMP levels in these cells using blue light prior to exposure to the oxygen gradient licensed the cells to detect and respond to the gradient to form a stable aerotactic band at some distance from the meniscus at 80 s postexposure (Fig. 3B). The aerotactic band formed by the cells under these conditions also formed farther away from the meniscus than the band formed by uninduced wild-type cells. Consistent with our above-described results, cells carrying pBlue-PDE formed an aerotactic band that was thinner than that formed by wild-type cells carrying pRed-DGC.

To confirm these observations, we performed a similar experiment using the *chsA* mutant carrying pBlue-PDE (Fig. 3C). This strain, exposed to green light, formed a stable aerotactic band 50 s after the introduction of the gradient. When the c-di-GMP levels in the *chsA*(pBlue-PDE) strain were decreased with a short pulse of blue light prior to exposure to the gradient, a stable aerotactic band was formed after 40 s. These results are consistent with c-di-GMP modulating the ability of the cells to locate the preferred oxygen concentration in the gradient. Since the swimming speed or reversal frequency of wild-type cells carrying pRed-DGC or pBlue-PDE did not change upon exposure to red or blue light, respectively (Tables 1 and 2), we interpret the changes in the time that it took cells to form a stable aerotactic band as reflecting differences in the abilities of the cells to respond to the gradient to which they were exposed.

We also analyzed the distribution of wild-type cells carrying pRed-DGC or pBlue-PDE, inside the capillary tubes, once a stable aerotactic band had formed (Fig. 3D). This analysis confirmed that wild-type cells containing pRed-DGC and exposed to red light accumulated as a sharp aerotactic band. There was also a visible zone of clearing on both sides of the aerotactic band, indicating a depletion of cells. The clearing zone was also larger on the side of the band closest to the meniscus, suggesting that these cells responded strongly to the increased oxygen concentrations compared to cells located at lower oxygen concentrations relative to the aerotactic band. Beyond this region, cells accumulated in a broad zone, producing a visibly denser hump, suggesting that cells failed to exhibit a strong and/or precise response to the gradient (Fig. 3D). The distribution of wild-type cells carrying pBlue-PDE and exposed to blue light was in stark contrast: fewer cells accumulated at the preferred position in the gradient, yielding a thin aerotactic band, and there was no clearing zone in the vicinity of the band. These observations suggest that these cells had only a weak response to the oxygen gradient. These results thus support the hypothesis that changes in c-di-GMP levels affect the ability of cells to both detect and accumulate at the preferred oxygen concentration in a gradient.

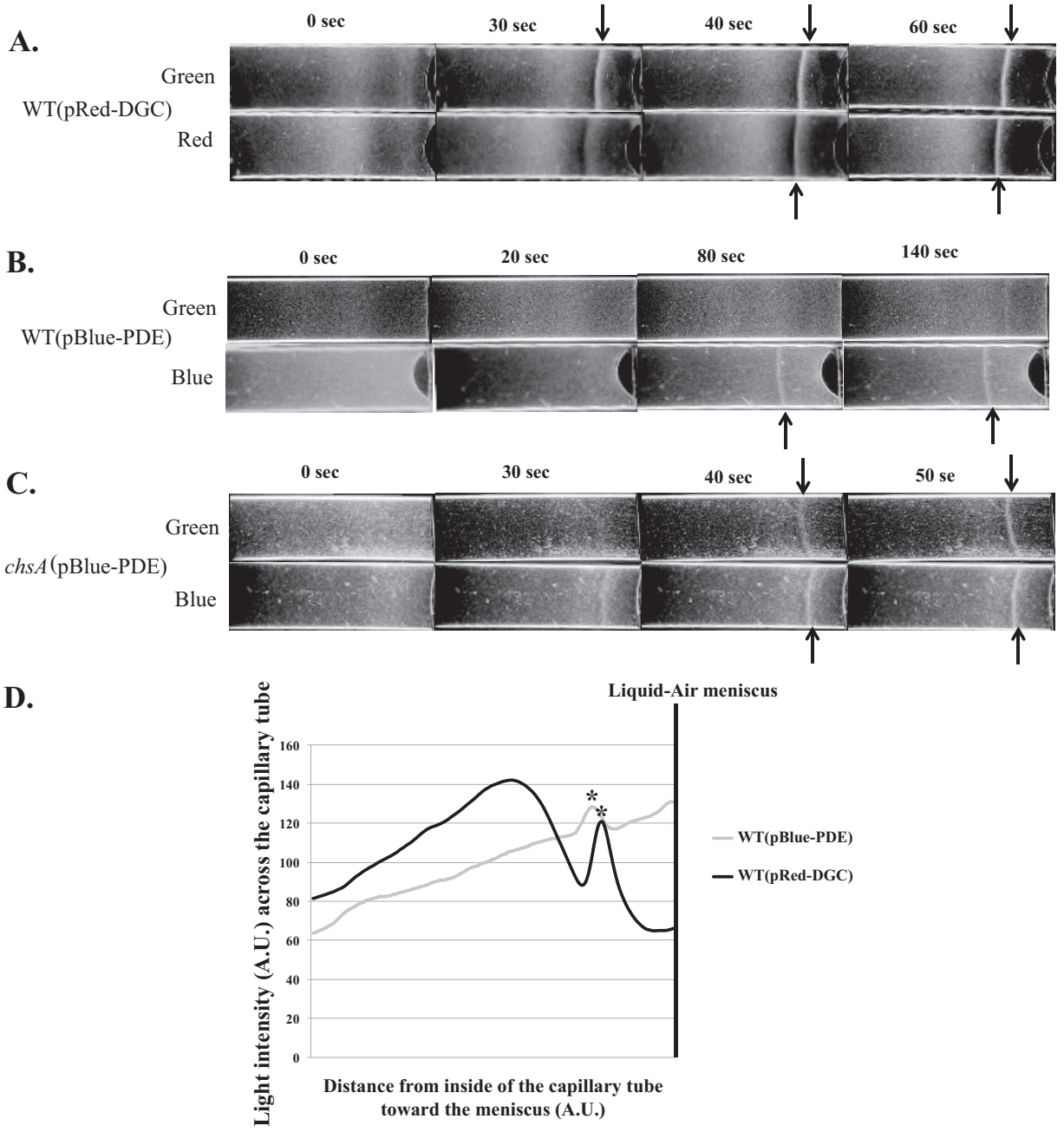

FIG 3 Effects of light-mediated changes in c-di-GMP levels on aerotaxis in spatial oxygen gradients. (A to C) Behavior of the WT strain carrying the optogenetic vectors pRed-DGC (A) and pBlue-PDE (B) in the gradient assay for aerotaxis, compared to that of the ChsA phosphodiesterase mutant (*chsA*) carrying pBlue-PDE (C). Cell suspensions standardized to equivalent numbers were placed into a capillary tube and exposed to N_2 for 3 min for equilibration under green light. Cells were next exposed to red or blue light for 10 s, and N_2 was immediately replaced with air that was allowed to flow into the chamber. Representative images of results from 3 biological replicates are shown. The time indicated at the top is in seconds after exposure to the air gradient. Arrows indicate the formation of a stable aerotactic band. (D) Distribution of cells throughout the capillary tubes after the formation of a stable aerotaxis band derived from image intensity analysis. The images of capillary tubes in which a stable aerotactic band formed under inducing conditions were analyzed by using ImageJ, as described in the text. Similar profiles were observed for biological replicates. A.U., arbitrary units.

Altering c-di-GMP levels affects the time to respond and adapt to an oxygen gradient. The results described above suggested that changes in c-di-GMP levels could affect the time that it took cells to form an aerotactic band and also excluded temporal changes in swimming speed in these behaviors. To further analyze this effect, we next determined the response time, which corresponds to the time that it takes motile cells stimulated with an attractant or repellent to return to a prestimulus swimming bias. The

TABLE 3 Effects of c-di-GMP on the time to adaptation of *A. brasilense* to temporal changes in aeration

	Avg adaptation time following a change in aeration (s) ± SE[b]			
	WT(pRed-DGC)		WT(pBlue-PDE)	
Condition[a]	Green light	Red light	Green light	Blue light
Air→N_2	23 ± 3	40 ± 2*	20 ± 1	29 ± 1*
N_2→air	31 ± 2	19 ± 1*	21 ± 1	17 ± 1*

[a]Direction of the temporal gradient of air of free-swimming cells observed.
[b]Shown are averages of data from three biological replicates with standard errors. * indicates a statistically significant difference from green light treatment ($P < 0.05$ by a *t* test).

response time varies with the nature of the effector (a stronger attractant/repellent causes the cells to modify their swimming bias for longer times) and the adaptation rate, which depends on the level of signaling activity of chemotaxis receptors (27–29). To test the possibility that c-di-GMP modulates the signaling activity, and, thus, the contribution, of receptors to aerotaxis, we measured the time to response of wild-type cells carrying pRed-DGC or pBlue-PDE to a temporal decrease or increase in oxygen concentrations, under noninducing (green light) or inducing (red or blue light) conditions (Table 3). We found that changing c-di-GMP levels affected the response time of cells carrying pRed-DGC or pBlue-PDE (Table 3). For air-adapted cells experiencing a decrease in oxygen concentrations (air to N_2), increased (pRed-DGC) or decreased (pBlue-PDE) c-di-GMP levels significantly increased the response time compared to that of noninduced cells (Table 3). In contrast, N_2-adapted cells experiencing an increase in oxygen concentrations (N_2 to air) responded to this temporal gradient by reducing the adaptation time compared to that of noninduced cells (Table 3). Consistent with the observed lag or lead time in aerotactic band formation seen for these cells (Fig. 3), these results suggest that modulating intracellular c-di-GMP levels directly alters the response time of cells in response to oxygen gradients and support the notion that c-di-GMP alters the signaling activity of the chemotaxis receptors involved.

Binding of c-di-GMP to a chemoreceptor, Tlp1, modulates its contribution to the aerotaxis response. The effects of c-di-GMP on the aerotaxis response seen here are expected to depend on signaling by a chemotaxis receptor(s). Several chemotaxis receptors mediate aerotaxis in *A. brasilense*, and only a few of them have been characterized to date (5, 30). To test the role of chemotaxis receptors, we introduced pRed-DGC into the *tlp1* mutant. We also introduced an empty vector (pRK415), a vector expressing parental Tlp1 (pRK-Tlp1), or a vector expressing a Tlp1 variant that is unable to bind c-di-GMP (pRK-Tlp1$^{R562A\ R563A}$) (5) into the *tlp1* mutant and analyzed band formation after the induction of c-di-GMP biosynthesis with red light (Fig. 4). Under noninducing green light, the *tlp1*(pRK415; pRed-DGC) strain formed an aerotactic band at some distance from the meniscus (654 ± 86 μm), 70 s after exposure to the gradient (Fig. 4A). The time that it took the cells to respond to the gradient and to form an aerotactic band was significantly different from that of wild-type cells under similar conditions (Fig. 3A). We previously showed that disrupting Tlp1 did not affect c-di-GMP metabolism (5), suggesting that the lack of functional Tlp1 caused the slower response of *tlp1*(pRK415; pRed-DGC) to the gradient. Increasing c-di-GMP levels with red light in the *tlp1*(pRK415; pRed-DGC) strain caused the band to form earlier as well as closer to the meniscus (405 ± 84 μm), with a stable band being formed 40 s after the introduction of the gradient (Fig. 4A). These effects were not caused by the presence of the pRK415 vector alone, since cells lacking this vector behaved in a similar fashion (data not shown). The expression of parental Tlp1 in the *tlp1* mutant [*tlp1*(pRK-Tlp1; pRed-DGC)] restored the timing of aerotactic band formation seen for the wild-type strain containing pRed-DGC (Fig. 4A and B). Furthermore, elevated c-di-GMP levels in the *tlp1*(pRK-Tlp1; pRed-DGC) strain with red light caused the aerotactic band to form later (>70 s post-gradient exposure) as well as further away from the meniscus (521 ± 57 μm) than under green light control conditions (339 ± 30 μm) (Fig. 4B). Cells of the

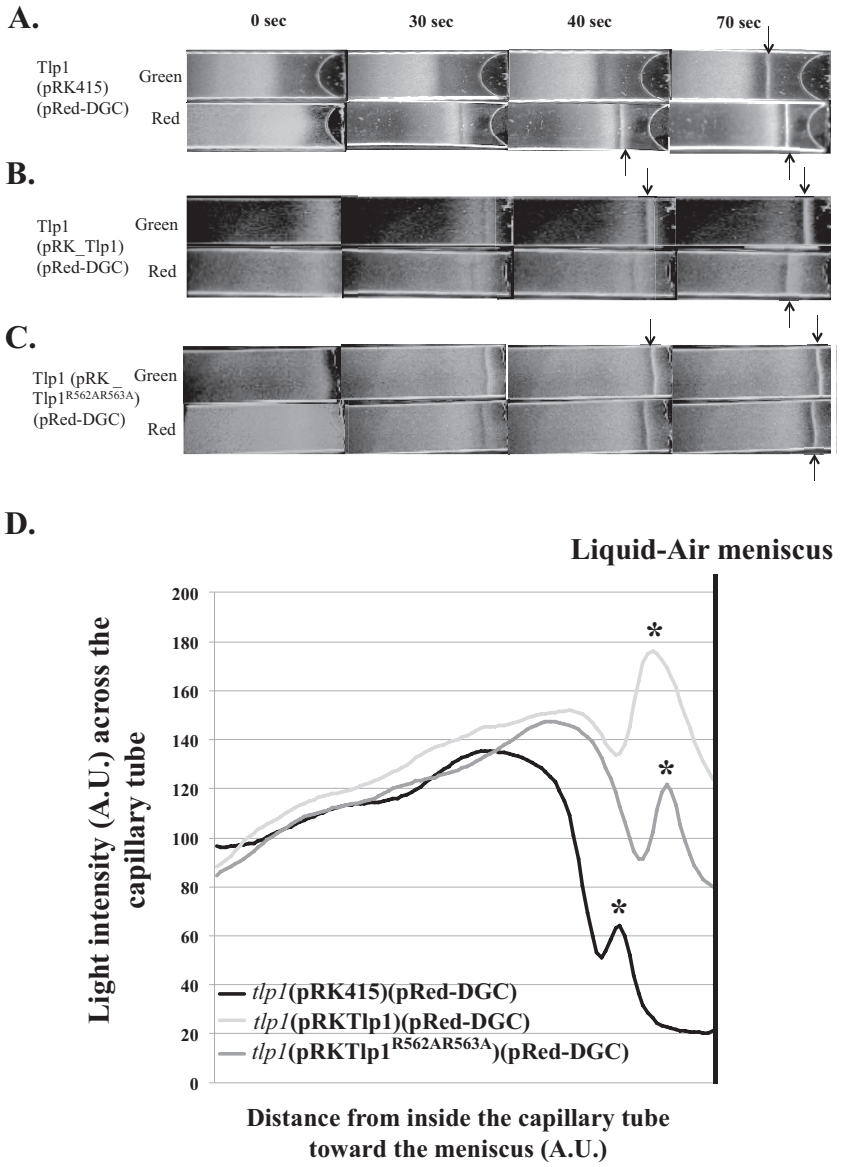

FIG 4 Role of Tlp1 c-di-GMP binding in mediating changes in sensitivity to oxygen gradients upon optogenetic manipulation of c-di-GMP levels. (A to C) Spatial gradient assays for aerotaxis using an *A. brasilense tlp1* mutant carrying the optogenetic vectors (pRed-DGC or pBlue-PDE) as well as an empty vector (pRK415) (A), parental Tlp1 (B), or a Tlp1 variant lacking residues for c-di-GMP binding ($Tlp1^{R562A\ R563A}$) (C). (D) Image analysis of the distribution of cells throughout the capillary tube after the formation of a stable aerotactic band. Cell suspensions standardized to equivalent numbers were placed into a capillary tube and exposed to N_2 for 3 min for equilibration under green light. Cells were then exposed to red or blue light for 10 s, and N_2 was immediately replaced with air that was allowed to flow into the chamber. Representative images of results from 3 biological replicates are shown. The time indicated at the top is in seconds after exposure to the air gradient. Arrows indicate the formation of a stable aerotactic band. Cells that had formed a band at the latest time points were selected for image analysis.

tlp1 mutant expressing $Tlp1^{R562A\ R563A}$ possess a Tlp1 receptor that is unable to bind c-di-GMP and formed a stable aerotactic band by 30 s under noninducing green light (Fig. 4C). Increasing c-di-GMP levels in this strain caused a small lag in the time that it took cells to form a stable aerotactic band (40 s), with the band also forming slightly farther away from the meniscus (490 $\pm$ 39 μm versus 341 $\pm$ 35 μm) (Fig. 4C). The formation of the aerotactic band at a specific position occurs within a reproducible time frame in cultures grown under similar conditions (7, 8, 23, 24). Therefore, these results suggest that the lack of functional Tlp1 as well as modulations of c-di-GMP levels

affected both the time to a response of the cells to the gradient as well as their ability to detect the preferred oxygen concentrations to accumulate as an aerotactic band.

We further compared the distributions of cells in the capillary tubes once the aerotactic band had formed (Fig. 4D). Both the *tlp1*(pRK415; pRed-DGC) and *tlp1*(pRKTlp1$^{R562A\ R563A}$; pRed-DGC) strains formed similar aerotactic bands characterized by a dense accumulation of cells at the position of the aerotactic band that was followed by a broad accumulation of cells at lower concentrations of oxygen relative to the aerotactic band. These results suggested that the behavior of cells lacking Tlp1 was similar to that of cells carrying Tlp1 that were unable to bind c-di-GMP, implying that binding of c-di-GMP to Tlp1 promotes the contribution of this receptor to the aerotaxis response. The accumulation of cells that failed to locate the position of the aerotactic band further supports this notion. Consistent with the role of Tlp1 in supporting aerotaxis, the distribution of *tlp1*(pRKTlp1; pRed-DGC) cells was characterized by a larger aerotactic band that seemed to comprise more cells, while little to no accumulation of cells behind this preferred position in the gradient was observed. These data indicate that binding of c-di-GMP to Tlp1 is required for the ability of cells to respond to the oxygen gradient, including the ability to shift the preferred position for accumulation as a band in the oxygen gradient.

c-di-GMP levels change with carbon metabolism. Aerotaxis is intimately linked to metabolism in *A. brasilense*, with the preferred position in an oxygen gradient corresponding to maximum intracellular energy production (8, 23, 31). We thus hypothesized that c-di-GMP could modulate the signaling contribution of some chemotaxis receptors as a function of metabolic status. This hypothesis implies that intracellular c-di-GMP concentrations vary with the carbon sources used for growth. Therefore, we first determined the c-di-GMP concentrations in wild-type cells grown in medium containing one of three preferred carbon sources for *A. brasilense* (8): malate, succinate, and fructose. Under conditions of growth in minimal medium, we found that intracellular c-di-GMP concentrations differed depending on the carbon source available for growth. Intracellular c-di-GMP levels were higher in cells grown on malate (2.7 $\pm$ 0.5 μM) and succinate (2.1 $\pm$ 0.7 μM) than in cells grown on fructose (1.3 $\pm$ 0.2 μM). Statistical analysis also indicated that c-di-GMP concentrations in fructose-grown cells were significantly different from the c-di-GMP levels detected in malate-grown cells (*P* value of $>$0.05). Doubling times were also lower on organic acids (4.3 $\pm$ 0.3 h for malate and 4.0 $\pm$ 0.4 h for succinate) than on fructose (6.2 $\pm$ 1.4 h), suggesting that different c-di-GMP levels could reflect different metabolic efficiencies. The average intracellular c-di-GMP concentrations that we obtained here were significantly higher under these conditions than those obtained with cells containing plasmids from the optogenetic system (Fig. 2). We note that in addition to carrying plasmids, which affect the growth rate, as we describe above, the cells were grown under different conditions, specifically, a rich medium (Fig. 2), compared to the minimal medium used here. We surmise that the distinct growth conditions and the presence of a plasmid together account for the discrepancy in intracellular c-di-GMP concentrations.

The dependence of *A. brasilense* aerotaxis on metabolism and the role of c-di-GMP in aerotaxis in this species, together with the results described above, suggested that changes in c-di-GMP levels could imprint the chemotaxis receptors of *A. brasilense* with a record of the cell's metabolic experience. We tested this hypothesis by comparing the preferred positions for aerotaxis band formation for the wild-type strain in the presence of various concentrations of malate or fructose. To evoke different metabolic experiences, we also used cells first grown on either malate or fructose (Fig. 5). As expected, the position of the aerotactic band in the oxygen gradient was sensitive to the nature and the concentration of the carbon source available for aerotaxis (Fig. 5A and B). There were striking differences between cells first grown on malate and cells first grown on fructose. First, the position of the aerotactic band formed by malate-grown cells changed depending on the concentration of the carbon source available for aerotaxis. In contrast, cells first grown on fructose formed an aerotactic band at similar locations

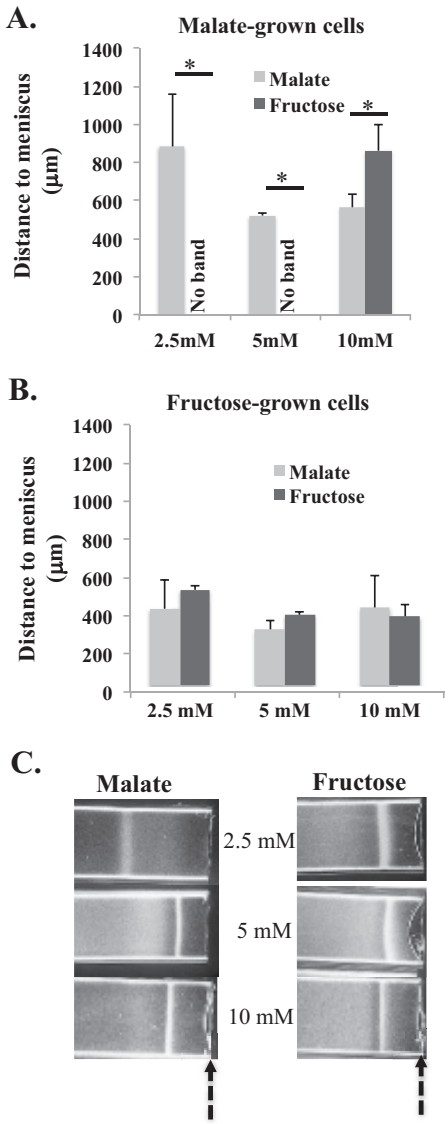

FIG 5 Effect of carbon source-mediated changes in c-di-GMP levels on the formation of an aerotactic band. (A) Average position of the stable aerotactic band relative to the air-liquid meniscus for wild-type cells grown on malate (10 mM), washed, and incubated with malate or fructose at different concentrations for the spatial gradient assay for aerotaxis. (B) Average position of the stable aerotactic band relative to the air-liquid meniscus for wild-type cells grown on fructose (10 mM), washed, and incubated with malate or fructose at different concentrations for the spatial gradient assay for aerotaxis. (C) Representative images of results from at least 3 replicates showing the position of the stable aerotactic band formed by *tlp1* mutant cells grown on malate (10 mM), washed, and incubated with malate or fructose at different concentrations for the spatial gradient assay for aerotaxis. The arrows indicate the position of the air-liquid meniscus. An asterisk represents a significant difference between samples (*P* value of <0.05).

in the oxygen gradient, regardless of the nature or the concentration of the carbon source available for aerotaxis (Fig. 5B). These observations suggest that cells that experienced recent conditions that caused elevated intracellular c-di-GMP levels (e.g., growth on malate) were able to adjust their aerotaxis response more precisely when they were subsequently exposed to an oxygen gradient. In contrast, cells that experienced conditions that decreased their c-di-GMP levels (e.g., growth on fructose) displayed an invariable subsequent aerotaxis response that was "blind" to changes in external conditions. Second, malate-grown cells failed to respond to the oxygen gradient in the presence of low concentrations of fructose, but they formed an aerotaxis band when higher concentrations of fructose were available for aerotaxis

(Fig. 5A). These results suggest that malate-grown cells rely on a more discriminative signaling input to select the preferred position for accumulation in a gradient by aerotaxis. This behavior would be expected if more receptors were contributing to the production of the aerotaxis response. In contrast, fructose-grown cells lacked the ability to fine-tune their preferred position for aerotaxis as a function of external conditions, as expected if fewer receptors were contributing to the signaling input (Fig. 5A). To further validate this hypothesis, we analyzed the aerotaxis response of the *tlp1* mutant under similar conditions (Fig. 5C). We found that the *tlp1* mutant first grown on malate was able to form an aerotactic band under all conditions, including low fructose concentrations. These data are consistent with Tlp1 contributing to the aerotaxis response of wild-type cells under these conditions and intracellular c-di-GMP levels altering the contribution of Tlp1 to the signaling output. Together, these findings suggest that c-di-GMP acts in a feedback loop that links recent metabolic experience to aerotaxis by affecting chemotaxis receptors such as Tlp1.

DISCUSSION

c-di-GMP is a second-messenger molecule in bacteria, and a range of assays and tools to characterize and manipulate c-di-GMP metabolism have been developed. Here, tools for manipulating c-di-GMP levels with high temporal resolution (seconds to minutes) have been tested. We adapted a recently engineered dichromatic optogenetic system for the real-time manipulation of c-di-GMP metabolism in bacteria (20) and used it to characterize the role of c-di-GMP signaling in the aerotaxis response of *A. brasilense*. We show that a brief induction of c-di-GMP biosynthesis, via a red-light-activated diguanylate cyclase, BphS, or the induction of c-di-GMP degradation via a blue-light-activated phosphodiesterase, EB1, leads to significant and transient changes in the c-di-GMP content of the cells within seconds. We also demonstrate that these transient changes are detected by the cells and affect the motility behavior in gradients of oxygen (aerotaxis). Specifically, we identify the binding of c-di-GMP to particular receptors as a mechanism to modulate the contribution of these receptors to the aerotaxis signaling output. Therefore, *A. brasilense* aerotaxis depends not only on signaling by dedicated chemotaxis receptors (5, 26, 30), as expected, but also on intracellular c-di-GMP levels.

We attribute the role of c-di-GMP in mediating changes in the aerotaxis response of *A. brasilense* to the ability of chemotaxis receptors, including Tlp1, to bind this molecule at its C-terminal PilZ domain. Mutants lacking Tlp1 or expressing a Tlp1 variant that is unable to bind c-di-GMP are not null for aerotaxis, which indicates that other receptors participate in this response and is consistent with previously reported findings (30, 32). The only other aerotaxis receptor for *A. brasilense* characterized to date is AerC, a soluble PAS domain-containing receptor that lacks a PilZ domain (30). AerC has a significant role in modulating the aerotaxis of cells grown under nitrogen fixation conditions, but it does not contribute to the aerotaxis response, including aerotactic band formation, of cells grown under nitrogen-replete conditions (30), which we used here. A total of 48 putative chemotaxis receptors are annotated in the genome of *A. brasilense*. In addition to Tlp1, there are four additional genes for chemotaxis receptors containing PilZ domains. These additional genes also encode proteins with predicted PAS domains and a protoglobin domain. Given that PAS and protoglobin domains are often involved in oxygen sensing, including instances where they are present in chemotaxis receptors (33, 34), it is possible that some of these *A. brasilense* receptors participate in aerotaxis alongside Tlp1.

The results obtained here are consistent with the binding of c-di-GMP to receptors, such as Tlp1, affecting the ability of cells to accumulate at a preferred position within a spatial gradient of oxygen. We propose that intracellular c-di-GMP levels dictate the contribution of target chemotaxis receptors to the chemotaxis signaling output. In support of this notion, we showed that the binding of c-di-GMP to Tlp1 was required to support aerotaxis at the level of the wild-type strain: a mutant strain expressing a Tlp1 variant that is unable to bind c-di-GMP behaved like the *tlp1* mutant strain, which

is consistent with previously reported findings (5). This further indicates that the binding of c-di-GMP to Tlp1 functions to increase the activity of this receptor. Our results show that changes in c-di-GMP levels occurring after an aerotactic band formed had little to no effect on the cell's behavior. This indicates that variation in the background levels of c-di-GMP does not affect the position of the aerotactic band once the cells have responded to the gradient. This is fully consistent with the lack of a role for c-di-GMP as an intracellular repellent or attractant and with the robustness of the chemotaxis response that is a hallmark of the behavior of *E. coli* (35–37).

Within a cell, chemotaxis receptors are incorporated into large polar chemotaxis arrays with no turnover and, thus, little change in chemotaxis receptor composition between cell divisions (38). To modulate the activity of receptors and their contribution to the signaling output, most bacteria regulate the activity of chemotaxis receptors through differential methylation (39, 40). Our findings that c-di-GMP levels modulated the contribution of specific receptors (Tlp1) to the signaling output indicate that diverse small molecules can serve as intracellular cues to alter the activity of chemotaxis receptors. Small-molecule binding domains other than PilZ are found at the extreme C termini of diverse chemotaxis receptors (5, 41). A review of the predicted or demonstrated ligand binding specificities for these domains suggests that Zn^{2+} (41) and oxygen (5) might also directly modulate the signaling contribution of some chemotaxis receptors as a function of oxidative stress or ambient oxygen concentrations, respectively. For modifying the receptors by methylation, cells tap in to the intracellular *S*-adenosylmethionine (SAM) pool as a source of methyl groups, which also serves as a source of methyl groups for many other biological molecules, thereby linking general metabolism with chemotaxis signaling. By using c-di-GMP to modify the activity of the chemotaxis receptors, cells use a second-messenger molecule that signals the transition between planktonic and sessile lifestyles. Thus, the nature of the metabolic signal that is embedded in SAM and in c-di-GMP is distinct and thus likely expands the ways in which cells ensure that their chemotaxis signaling activity is fine-tuned with metabolism.

The formation of the tight aerotactic band at preferred, yet variable, positions in an oxygen gradient is reminiscent of the precision sensing behavior displayed during thermotaxis in *E. coli* (42, 43). During thermotaxis, *E. coli* cells do not simply move up or down a temperature gradient but sense a particular temperature, and this behavior depends on chemotaxis receptor activity, set by differential methylation (44, 45). If aerotaxis is a form of precision sensing, then the accumulation of cells in the aerotactic band at a preferred position in the gradient is the result of the antagonistic signaling of receptors that sense oxygen (or a related cue such as redox) as an attractant versus those that sense oxygen as a repellent (or a related cue such as redox), with the summation of their signaling inputs ultimately determining the preferred position of the aerotaxis band in the gradient. This is consistent with data from previous experiments and mathematical modeling predictions (23, 24) that suggest that the formation of a stable aerotactic band in spatial gradients of oxygen by motile *A. brasilense* cells results from the ability of these cells to sense high and low oxygen concentrations as repellents and a precise, very low oxygen concentration as an attractant signal. The low oxygen concentration was estimated to be 0.4% dissolved oxygen when cells use malate as a carbon source (23). The effects of c-di-GMP on the position of the aerotactic band and on modulating the contribution of Tlp1 to aerotaxis together suggest that this molecule could tip the balance between the antagonistic activities of oxygen (or related cues)-sensing receptors implicated in determining the location of the preferred oxygen concentration in the gradient. Given that aerotaxis allows *A. brasilense* to locate positions in the gradients where energy generation via metabolism is maximal (23), this further suggests that c-di-GMP signals a particular metabolic status. In agreement with this hypothesis, the intracellular c-di-GMP levels changed with growth on different carbon sources and affected the ability of cells to locate the preferred oxygen concentration when cells were then exposed to an oxygen gradient. Our results also suggest that intracellular c-di-GMP levels may function in a feedback loop to imprint the

chemotaxis machinery with a "memory" of recent metabolic experience: cells that experienced growth on a readily metabolizable substrate, such as malate, adjusted their preferred position in the oxygen gradient depending on prevailing conditions, while cells that experienced lower growth rates prior to exposure to the gradient, such as growth on fructose, did not compute the prevailing conditions in determining their preferred position in the oxygen gradient. Given that this effect was linked to the signaling activity of Tlp1, the effect of c-di-GMP on increasing or decreasing the contribution of specific receptors to aerotaxis could thus provide a straightforward mechanism to tightly couple past metabolic experience with current metabolic status to ensure optimum energy generation by aerotaxis. Our observations that increased or decreased c-di-GMP levels affect the time that it took cells to respond to temporal changes in oxygen concentrations in the atmosphere directly support this notion and are consistent with aerotaxis being a metabolism-dependent behavior (5, 8, 33). In most bacteria studied to date, c-di-GMP is a major cue for signaling the transition from planktonic to sessile lifestyles, and this transition typically occurs as a result of metabolic challenges. It is thus not surprising to find a link between c-di-GMP levels and metabolism. The recent finding that a single-domain PilZ protein can modulate the activity of a chemotaxis-specific methyltransferase to control receptor signaling and chemotaxis in *Pseudomonas aeruginosa* (46) suggests that the mechanism that we suggest here is not unique to *A. brasilense*.

The dependence of c-di-GMP levels on carbon sources and, possibly, growth rates was also reported previously for *Vibrio cholerae* (47). Many other environmental cues, in addition to carbon sources, regulate c-di-GMP levels in bacteria, including oxygen, temperature, light, and amino acids (5, 48–50). It is thus possible that other small molecules also alter the contribution of chemotaxis receptors to the signaling output.

MATERIALS AND METHODS

Bacterial strains and growth conditions. The wild-type Sp7 strain of *A. brasilense* and its *tlp1* mutant derivative (strain SG323) (32) were used throughout this study (see Table S1 in the supplemental material). Cells were grown in the dark at 28°C with shaking in minimal medium for *A. brasilense* (MMAB) containing 10 mM malate as a carbon source. In experiments with different carbon sources, cells were grown with shaking in minimal medium with 10 mM fructose or 10 mM succinate. All culture stocks were maintained on MMAB containing 1.5% agar with the following appropriate antibiotics: ampicillin (200 μg/ml), kanamycin (30 μg/ml), and/or tetracycline (10 μg/ml).

To determine doubling times, precultures were grown to stationary phase (optical density at 600 nm [OD_{600}] of 1) in MMAB containing 10 mM malate, succinate, or fructose as the sole carbon source. A 96-well microplate was prepared with MMAB containing 10 mM malate, succinate, or fructose, and wells were inoculated with a 1:10 dilution of the precultures. The absorbance at 600 nm was recorded every 20 min for 20 h by using a BioTech Synergy 2 microplate reader with Gen5 2.09 Read Control and Data Analysis software. Doubling times were calculated as time/generations, and the number of generations was calculated by using the formula $[\log (N_t/N_0)]/0.3$, where N_t is the OD_{600} at the end of log phase, N_0 is the OD_{600} at the beginning of log phase, and time is the time that elapsed between N_t and N_0.

Plasmid construction. The plasmids for the optogenetic regulation of intracellular c-di-GMP levels were constructed by using the vector pIND4, which carries two replication origins, ColE1 for *E. coli* and pMG160 for alphaproteobacteria (31). The *bphS-bphO* fragment from plasmid pMQbSH (21) that expresses the red/near-infrared-light-dependent diguanylate cyclase BphS and the heme oxygenase BphO was ligated into pIND4 digested with XbaI and BamHI to yield pRed-DGC. In this plasmid, *bphS* and *bphO* are arranged in an operon that is expressed from the IPTG-inducible P_{lac} promoter. The three-gene *bphS-bphO-eb1* operon containing, in addition to *bphS* and *bphO*, the *eb1* gene encoding a blue-light-activated PDE was amplified from plasmid pbSHE (20) and cloned into pIND4 digested with XbaI and BamHI to yield plasmid pBlue-PDE.

Transfer of plasmid-borne light-activated constructs into *A. brasilense*. To transfer pIND4, pBlue-PDE, or pRed-DGC, biparental conjugation was utilized, as previously described (51), with *Escherichia coli* strain S17.1 containing the plasmid of interest as a donor and *A. brasilense* strain Sp7 or its *tlp1* mutant derivative as a recipient. The presence of the plasmid in transconjugants grown on selective medium was confirmed by colony PCR, where the *lacI* gene, which is specific to the plasmid, was amplified by using primers pIND4-LacIq-Fwd (5′-GTGGTGAATGTGAAACCAGT-3′) and pIND4-LacIq-Rev (5′-TCACTGCCCGCTTTCCAGTC-3′).

Quantification of c-di-GMP concentrations by mass spectrometry. For the determination of whole-cell intracellular c-di-GMP concentrations, *A. brasilense* was grown in tryptone-yeast (TY) medium in the dark until the OD_{600} reached 1.0. Cultures were then reinoculated into TY medium and grown to an OD_{600} of 0.8. c-di-GMP was extracted, and the concentration was analyzed by using liquid chromatography-tandem mass spectrometry (LC-MS/MS) at the Michigan State University Mass Spectrometry and Metabolomics Core, as previously described (51, 52). The intracellular c-di-GMP concen-

tration was determined by dividing the total amount of c-di-GMP determined by LC-MS/MS by the number of cells, which was derived from plating assays, and by the volume of an *A. brasilense* cell, which was determined as previously described (47).

Behavior of free-swimming cells and computerized assisted motion tracking. Cells were grown to an OD_{600} of 0.6 to 0.7 (exponential growth phase) in MMAB containing 10 mM malate. Cultures were standardized to an equivalent number of cells, washed, and concentrated 10 times in Che buffer (1.7 g liter^{-1} dipotassium phosphate, 1.36 g liter^{-1} monopotassium phosphate, 0.1 mM EDTA). Under these conditions, at least 80% of cells are motile. Cells were exposed to green light (505 to 575 nm) for 1 min, exposed to either red light (610 to 730 nm) or blue light (450 nm) for 10 s, and then returned to green light. Digital recording of cell behavior continued throughout the experiment and lasted at least 5 min after the stimulus. Andover optical dichroic filters were used for exposure to green, red, and blue light. All swimming assays were filmed by using a 40× objective of a phase-contrast microscope fitted with a Leica MP120 HD digital camera. Videos were formatted by using VLC media player software before using CellTrak version 1.5 (Motion Analysis Corp., Santa Rosa, CA) for swimming speed and reversal frequency analyses. One-second segments (30 frames) of video were analyzed before, during, and after the stimulus pulse. At least 100 cells per time point were analyzed, and only motile cells were used for analysis.

Spatial gradient assay for aerotaxis and density analyses. Cells were grown to an OD_{600} of 0.6 to 0.7 in the dark in minimal medium containing malate. Cultures were standardized under green light, as described above. The concentrated sample was then used to fill a 0.1- by 1-mm capillary tube (Vitro Dynamics, Inc., Rockaway, NJ). Capillary tubes were placed into a gas equilibration chamber (31). Samples were allowed to equilibrate in humidified N_2 for 2 min inside the capillary tube under green light exposure. After equilibration, samples were exposed to either red or blue light for 10 s, nitrogen gas was turned off, and air was allowed to flow into the chamber. Aerotaxis was observed under green light for an additional 5 min. Images were captured by using the 4× objective of a phase-contrast Nikon E200 microscope and a C-mounted Nikon Coolpix digital camera. The distance from the meniscus and width of the aerotactic band were quantified by using the measure tool in FIJI in ImageJ. The width of the tube was used as a reference for all measurements. The distance from the meniscus was measured from the center of the meniscus to the center of the aerotactic band, and the width of the aerotactic band was measured at the middle of the band upon the formation of a stable band. The distribution of bacteria in capillary tubes was analyzed by intensity image analysis from digital pictures of aerotactic bands, using surface plot in ImageJ (http://imagej.nih.gov/) after Gaussian adjustment.

Temporal gradient for aerotaxis and analysis of swimming patterns. Cells were grown to an OD_{600} of 0.6 and washed with Che buffer before being concentrated 10 times in the same buffer. Ten microliters of the concentrated sample was placed onto a slide inside a gas equilibration chamber (31). All cells used for analysis were motile and free swimming. Air or humidified N_2 was allowed to flow over the cells for 3 min. After equilibration, the atmosphere of the cells was switched to N_2 or air, respectively, thereby producing the stimulatory temporal gradient of oxygen. Under these conditions, free-swimming cells suppress reversals during the transition from N_2 to air or air to N_2, since the microaerobic oxygen conditions experienced by cells during these transitions are attractants for *A. brasilense* (31). When c-di-GMP metabolism was also manipulated in the temporal aerotaxis assay, wild-type cells carrying pRed-DGC, pBlue-DGC, or pIND4 were first equilibrated in air or N_2 for 3 min, exposed to red or blue light for 10 s, and then immediately exposed to N_2 or air, respectively. All assays were recorded by using a 40× objective of a phase-contrast microscope fitted with a Leica MP120 HD digital camera. Blind video analysis was used to determine the response time, i.e., the time required for the cell population to return to the prestimulus swimming bias, following changes in aeration conditions. Short segments of recordings were also analyzed by computerized motion analysis (CellTrak 2.0) to verify the measurements. The response time was defined as the amount of time that it took 50% of cells to return to a prestimulus reversal frequency.

Cell clumping and aggregation analysis. The *chsA* mutant carrying pIND4 or pBlue-PDE was grown in the dark to an OD_{600} of 0.6, washed, and concentrated as described above. Ten microliters of the concentrated sample was placed onto a slide, and cells were allowed to swim freely. Cells were exposed to green light for 3 min and then exposed to either red or blue light for 10 s. After exposure, cells were placed back under green light. Images of the cell suspension were taken before and after exposure to red or blue light. The area covered by the clumps relative to the total surface area imaged was calculated by using the area measure tool in FIJI in ImageJ and used to determine the fold change in the surface areas covered by clumps.

Statistical analysis of data. To compare the effects of increases or decreases in c-di-GMP concentrations using the optogenetic system and the different growth conditions on the intracellular c-di-GMP concentration or the swimming speed and reversal frequency, analysis of variance (ANOVA) with a *post hoc* test (*P* value of 0.05) (Excel; Microsoft, Inc.) was used.

SUPPLEMENTAL MATERIAL

Supplemental material for this article may be found at https://doi.org/10.1128/JB.00020-17.

SUPPLEMENTAL FILE 1, PDF file, 5.4 MB.

ACKNOWLEDGMENTS

We thank Yann Dufour (Michigan State University) for insightful suggestions regarding aerotaxis band formation.

This work was supported by NSF grant MCB 13330344 to G.A. and in part by NSF grant MCB 1052575 to M.G. L.O. was supported by R25GM086761.

Any opinions, findings, conclusions, or recommendations expressed in this material are those of the authors and do not necessarily reflect the views of the National Science Foundation.

REFERENCES

1. Römling U, Galperin MY, Gomelsky M. 2013. Cyclic di-GMP: the first 25 years of a universal bacterial secondary messenger. Microbiol Mol Biol Rev 77:1–52. https://doi.org/10.1128/MMBR.00043-12.
2. Ryjenkov DA, Simm R, Romling U, Gomelsky M. 2006. The PilZ domain is a receptor for the second messenger c-di-GMP: the PilZ domain protein YcgR controls motility in enterobacteria. J Biol Chem 281:30310–30314. https://doi.org/10.1074/jbc.C600179200.
3. Amikam D, Galperin MY. 2006. PilZ domain is part of the bacterial c-di-GMP binding protein. Bioinformatics 22:3–6. https://doi.org/10.1093/bioinformatics/bti739.
4. Benach J, Swaminathan SS, Tamayo R, Handelman SK, Folta-Stogniew E, Ramos JE, Forouhar F, Neely H, Seetharaman J, Camilli A, Hunt JF. 2007. The structural basis of cyclic diguanylate signal transduction by PilZ domains. EMBO J 26:5153–5166. https://doi.org/10.1038/sj.emboj.7601918.
5. Russell MH, Bible AN, Fang X, Gooding JR, Campagna SR, Gomelsky M, Alexandre G. 2013. Integration of the second messenger c-di-GMP into the chemotactic signaling pathway. mBio 4:e00001-13. https://doi.org/10.1128/mBio.00001-13.
6. Hazelbauer GL, Lai WC. 2010. Bacterial chemoreceptors: providing enhanced features to two-component signaling. Curr Opin Microbiol 13:124–132. https://doi.org/10.1016/j.mib.2009.12.014.
7. Alexandre G, Greer-Phillips S, Zhulin I. 2004. Ecological role of energy taxis in microorganisms. FEMS Microbiol Rev 28:113–126. https://doi.org/10.1016/j.femsre.2003.10.003.
8. Alexandre G, Greer SE, Zhulin IB. 2000. Energy taxis is the dominant behavior in *Azospirillum brasilense*. J Bacteriol 182:6042–6048. https://doi.org/10.1128/JB.182.21.6042-6048.2000.
9. Bible AN, Stephens BB, Ortega DR, Xie Z, Alexandre G. 2008. Function of a chemotaxis-like signal transduction pathway in modulating motility, cell clumping, and cell length in the alphaproteobacterium *Azospirillum brasilense*. J Bacteriol 190:6365–6375. https://doi.org/10.1128/JB.00734-08.
10. Wisniewski-Dye F, Borziak K, Khalsa-Moyers G, Alexandre G, Sukharnikov LO, Wuichet K, Hurst GB, McDonald WH, Robertson JS, Barbe V, Calteau A, Rouy Z, Mangenot S, Prigent-Combaret C, Normand P, Boyer M, Siguier P, Dessaux Y, Elmerich C, Condemine G, Krishnen G, Kennedy I, Paterson AH, Gonzalez V, Mavingui P, Zhulin IB. 2011. *Azospirillum* genomes reveal transition of bacteria from aquatic to terrestrial environments. PLoS Genet 7:e1002430. https://doi.org/10.1371/journal.pgen.1002430.
11. Carreno-Lopez R, Sanchez A, Camargo N, Elmerich C, Baca BE. 2009. Characterization of *chsA*, a new gene controlling the chemotactic response in *Azospirillum brasilense* Sp7. Arch Microbiol 191:501–507. https://doi.org/10.1007/s00203-009-0475-x.
12. Ramirez-Mata A, Lopez-Lara LI, Xiqui-Vazquez ML, Jijon-Moreno S, Romero-Osorio A, Baca BE. 2016. The cyclic-di-GMP diguanylate cyclase CdgA has a role in biofilm formation and exopolysaccharide production in *Azospirillum brasilense*. Res Microbiol 167:190–201. https://doi.org/10.1016/j.resmic.2015.12.004.
13. Kulasakara H, Lee V, Brencic A, Liberati N, Urbach J, Miyata S, Lee DG, Neely AN, Hyodo M, Hayakawa Y, Ausubel FM, Lory S. 2006. Analysis of *Pseudomonas aeruginosa* diguanylate cyclases and phosphodiesterases reveals a role for bis-(3′-5′)-cyclic-GMP in virulence. Proc Natl Acad Sci U S A 103:2839–2844. https://doi.org/10.1073/pnas.0511090103.
14. Le Guyon S, Simm R, Rehn M, Romling U. 2015. Dissecting the cyclic di-guanylate monophosphate signalling network regulating motility in *Salmonella enterica* serovar Typhimurium. Environ Microbiol 17:1310–1320. https://doi.org/10.1111/1462-2920.12580.
15. Ha DG, Richman ME, O'Toole GA. 2014. Deletion mutant library for investigation of functional outputs of cyclic diguanylate metabolism in *Pseudomonas aeruginosa* PA14. Appl Environ Microbiol 80:3384–3393. https://doi.org/10.1128/AEM.00299-14.
16. Gao X, Dong X, Subramanian S, Matthews PM, Cooper CA, Kearns DB, Dann CE, III. 2014. Engineering of *Bacillus subtilis* strains to allow rapid characterization of heterologous diguanylate cyclases and phosphodiesterases. Appl Environ Microbiol 80:6167–6174. https://doi.org/10.1128/AEM.01638-14.
17. Abel S, Fau BT, Nicollier M, Hug I, Kaever V, Abel Zur Wiesch P, Jenal U. 2013. Bi-modal distribution of the second messenger c-di-GMP controls cell fate and asymmetry during the caulobacter cell cycle. PLoS Genet 9:e1003744. https://doi.org/10.1371/journal.pgen.1003744.
18. Christen M, Kulasekara HD, Christen B, Kulasekara BR, Hoffman LR, Miller SI. 2010. Asymmetrical distribution of the second messenger c-di-GMP upon bacterial cell division. Science 328:1295–1297. https://doi.org/10.1126/science.1188658.
19. Lori C, Ozaki S, Steiner S, Bohm R, Abel S, Dubey BN, Schirmer T, Hiller S, Jenal U. 2015. Cyclic di-GMP acts as a cell cycle oscillator to drive chromosome replication. Nature 523:236–239. https://doi.org/10.1038/nature14473.
20. Ryu M-H, Fomicheva A, Moskvin OV, Gomelsky M. 2017. Optogenetic module for dichromatic control of cyclic di-GMP signaling. J Bacteriol 199:e00014-17. https://doi.org/10.1128/JB.00014-17.
21. Ryu M-H, Gomelsky M. 2014. Near-infrared light responsive synthetic c-di-GMP module for optogenetic applications. ACS Synth Biol 3:802–810. https://doi.org/10.1021/sb400182x.
22. Ind AC, Porter SL, Brown MT, Byles ED, de Beyer JA, Godfrey SA, Armitage JP. 2009. Inducible-expression plasmid for *Rhodobacter sphaeroides* and *Paracoccus denitrificans*. Appl Environ Microbiol 75:6613–6615. https://doi.org/10.1128/AEM.01587-09.
23. Zhulin IB, Bespalov VA, Johnson MS, Taylor BL. 1996. Oxygen taxis and proton motive force in *Azospirillum brasilense*. J Bacteriol 178:5199–5204. https://doi.org/10.1128/jb.178.17.5199-5204.1996.
24. Mazzag BC, Zhulin IB, Mogilner A. 2003. Model of bacterial band formation in aerotaxis. Biophys J 85:3558–3574. https://doi.org/10.1016/S0006-3495(03)74775-4.
25. Bible AN, Russell MH, Alexandre G. 2012. The *Azospirillum brasilense* Che1 chemotaxis pathway controls swimming velocity, which affects transient cell-to-cell clumping. J Bacteriol 194:3343–3355. https://doi.org/10.1128/JB.00310-12.
26. Mukherjee T, Kumar D, Burriss N, Xie Z, Alexandre G. 2016. *Azospirillum brasilense* chemotaxis depends on two signaling pathways regulating distinct motility parameters. J Bacteriol 198:1764–1772. https://doi.org/10.1128/JB.00020-16.
27. Berg H, Brown D. 1972. Chemotaxis in *Escherichia coli* analysed by three dimensional tracking. Nature 239:500–504. https://doi.org/10.1038/239500a0.
28. Berg H, Tedesco P. 1975. Transient response to chemotactic stimuli in *Escherichia coli*. Proc Natl Acad Sci U S A 72:3235–3239. https://doi.org/10.1073/pnas.72.8.3235.
29. Meir Y, Jakovlejevic V, Oleksiuk O, Sourjik V, Wingreen N. 2010. Precision and kinetics of adaptation in bacterial chemotaxis. Biophys J 99:2766–2774. https://doi.org/10.1016/j.bpj.2010.08.051.
30. Xie Z, Ulrich L, Zhulin I, Alexandre G. 2010. PAS domain containing chemoreceptor couples dynamic changes in metabolism with chemotaxis. Proc Natl Acad Sci U S A 107:2235–2240. https://doi.org/10.1073/pnas.0910055107.
31. Zhulin IB, Armitage JP. 1993. Motility, chemokinesis, and methylation-independent chemotaxis in *Azospirillum brasilense*. J Bacteriol 175:952–958. https://doi.org/10.1128/jb.175.4.952-958.1993.
32. Greer-Phillips S, Stephens B, Alexandre G. 2004. An energy taxis transducer promotes root colonization by *Azospirillum brasilense*. J Bacteriol 186:6595–6604. https://doi.org/10.1128/JB.186.19.6595-6604.2004.
33. Alexandre G. 2010. Coupling metabolism and chemotaxis-dependent behaviours by energy taxis receptors. Microbiology 156:2283–2293. https://doi.org/10.1099/mic.0.039214-0.
34. Henry JT, Crosson S. 2011. Ligand-binding PAS domains in a genomic,

cellular, and structural context. Annu Rev Microbiol 65:261–286. https://doi.org/10.1146/annurev-micro-121809-151631.
35. Alon U, Surette MG, Barkai N, Leibler S. 1999. Robustness in bacterial chemotaxis. Nature 397:168–171. https://doi.org/10.1038/16483.
36. Yi T-M, Huang Y, Simon MI, Doyle J. 2000. Robust perfect adaptation in bacterial chemotaxis through integral feedback control. Proc Natl Acad Sci U S A 97:4649–4653. https://doi.org/10.1073/pnas.97.9.4649.
37. Lazova MD, Ahmed T, Bellomo D, Stocker R, Shimizu TS. 2011. Response rescaling in bacterial chemotaxis. Proc Natl Acad Sci U S A 108:13870–13875. https://doi.org/10.1073/pnas.1108608108.
38. Schulmeister S, Ruttorf M, Thiem S, Kentner D, Lebiedz D, Sourjik V. 2008. Protein exchange dynamics at chemoreceptor clusters in *Escherichia coli*. Proc Natl Acad Sci U S A 105:6403–6408. https://doi.org/10.1073/pnas.0710611105.
39. Levit MN, Stock JB. 2002. Receptor methylation controls the magnitude of stimulus-response coupling in bacterial chemotaxis. J Biol Chem 277:36760–36765. https://doi.org/10.1074/jbc.M204325200.
40. Weis RM, Koshland DE. 1988. Reversible receptor methylation is essential for normal chemotaxis of *Escherichia coli* in gradients of aspartic acid. Proc Natl Acad Sci U S A 85:83–87. https://doi.org/10.1073/pnas.85.1.83.
41. Draper J, Karplus K, Otterman KM. 2011. Identification of a chemoreceptor zinc-binding domain common to cytoplasmic bacterial chemoreceptors. J Bacteriol 193:4338–4345. https://doi.org/10.1128/JB.05140-11.
42. Oleksiuk O, Jakovljevic V, Vladimirov N, Carvalho R, Paster E, Ryu WS, Meir Y, Wingreen NS, Kollmann M, Sourjik V. 2011. Thermal robustness of signaling in bacterial chemotaxis. Cell 145:312–321. https://doi.org/10.1016/j.cell.2011.03.013.
43. Salman H, Libchaber A. 2007. A concentration-dependent switch in the bacterial response to temperature. Nat Cell Biol 9:1098–1100. https://doi.org/10.1038/ncb1632.
44. Jiang L, Ouyang Q, Tu Y. 2009. A mechanism for precision-sensing via a gradient-sensing pathway: a model of *Escherichia coli* thermotaxis. Biophys J 97:74–82. https://doi.org/10.1016/j.bpj.2009.04.029.
45. Micali G, Endres RG. 2016. Bacterial chemotaxis: information processing, thermodynamics, and behavior. Curr Opin Microbiol 30:8–15. https://doi.org/10.1016/j.mib.2015.12.001.
46. Xu L, Xin L, Zeng Y, Yam JKH, Ding Y, Venkataramani P, Cheang QW, Yang X, Tang X, Zhang L-H, Chiam K-H, Yang L, Liang Z-X. 2016. A cyclic di-GMP-binding adaptor protein interacts with a chemotaxis methyltransferase to control flagellar motor switching. Sci Signal 9:ra102. https://doi.org/10.1126/scisignal.aaf7584.
47. Koestler BJ, Waters CM. 2013. Exploring environmental control of cyclic di-GMP signaling in *Vibrio cholerae* by using the *ex vivo* cyclic di-GMP assay (TELCA). Appl Environ Microbiol 79:5233–5241. https://doi.org/10.1128/AEM.01596-13.
48. Bernier SP, Ha D-G, Khan W, Merritt JH, O'Toole GA. 2011. Modulation of *Pseudomonas aeruginosa* surface-associated group behaviors by individual amino acids through c-di-GMP signaling. Res Microbiol 162:680–688. https://doi.org/10.1016/j.resmic.2011.04.014.
49. Ryan RP, Fouhy Y, Lucey JF, Jiang B-L, He Y-Q, Feng J-X, Tang J-L, Dow JM. 2007. Cyclic di-GMP signalling in the virulence and environmental adaptation of *Xanthomonas campestris*. Mol Microbiol 63:429–442. https://doi.org/10.1111/j.1365-2958.2006.05531.x.
50. Townsley L, Yildiz FH. 2015. Temperature affects c-di-GMP signalling and biofilm formation in *Vibrio cholerae*. Environ Microbiol 17:4290–4305. https://doi.org/10.1111/1462-2920.12799.
51. Vanstockem MMK, Vanderleyden J, Van Gool AP. 1987. Transposon mutagenesis of *Azospirillum brasilense* and *Azospirillum lipoferum*: physical analysis of Tn*5* and Tn*5*-Mob insertion mutants. Appl Environ Microbiol 53:410–415.
52. Bobrov AG, Fau KO, Ryjenkov DA, Waters CM, Price PA, Fetherston JD, Mack D, Goldman WE, Gomelsky M, Perry RD. 2011. Systematic analysis of cyclic di-GMP signaling enzymes and their role in biofilm formation and virulence in *Yersinia pestis*. Mol Microbiol 79:533–551. https://doi.org/10.1111/j.1365-2958.2010.07470.x.